Electronic Supplementary Material (ESI) for Inorganic Chemistry Frontiers.

Electrocatalytic Production of Hydrogen Peroxide Enabled by Post-Synthetic Modification of a Self-Assembled Porphyrin Cube

Matthew R. Crawley, Daoyang Zhang, and Timothy R. Cook*

[a] *Department of Chemistry, University at Buffalo, The State University of New York, Buffalo, New York 14260, United States.*

Supplementary Information

Contents

NMR:

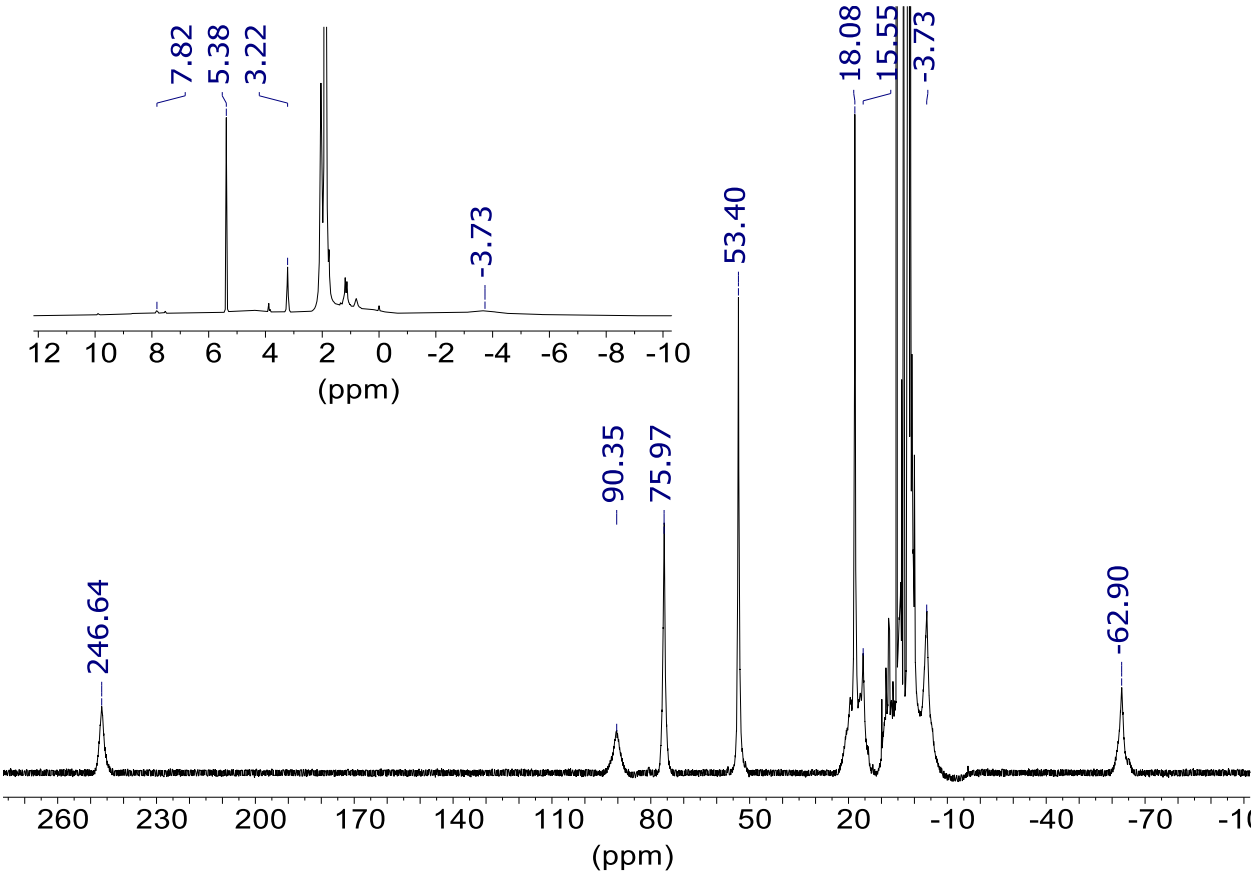

Figure S1.Paramagnetic ^{1}H NMR of **CoCo-cube**. *(500 MHz, CD_3CN, 25°C).*

High-Resolution Mass Spectrometry:

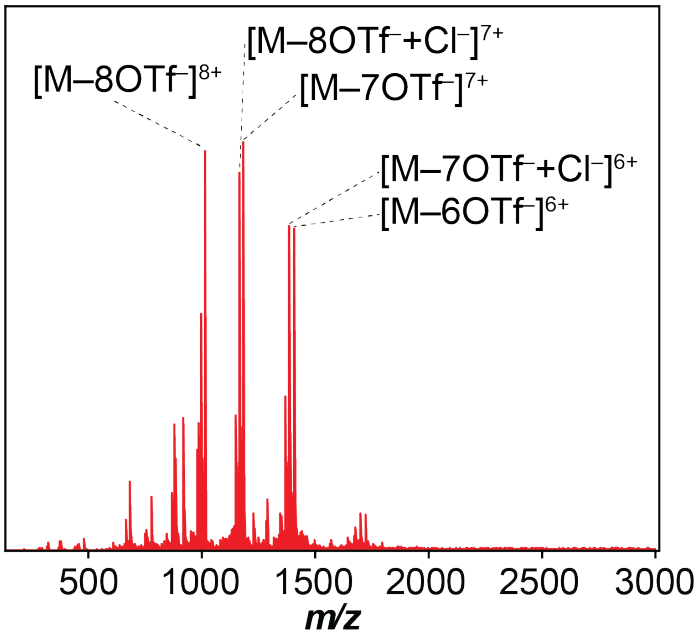

Figure S2. ESI-FT-ICR high resolution mass spectrum of **FeCu-cube** acquired in CH_3CN in positive mode. M = $(C_{408}H_{264}Cu_6Fe_8N_{72})(OTf)_{16}$.

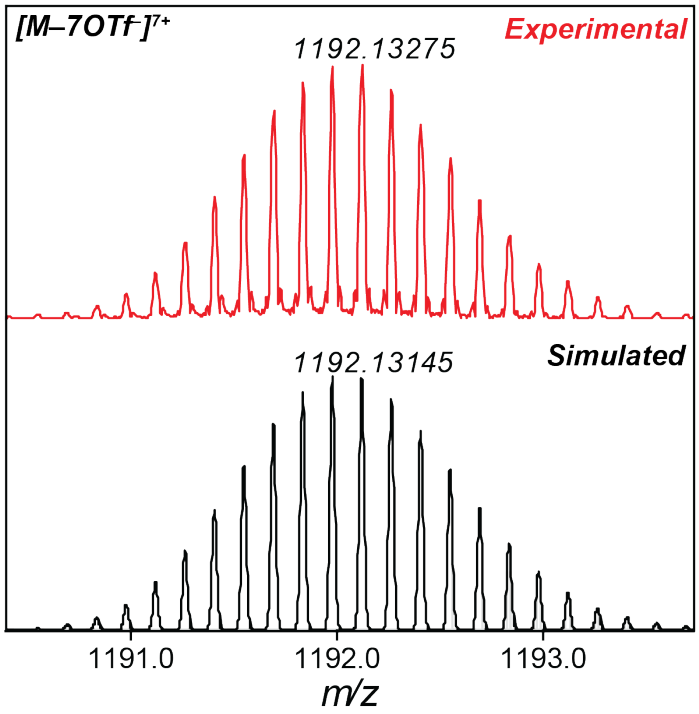

Figure S3. The 7+ base peak in Figure S2 corresponding (top) Experimental data, (bottom) simulated spectrum with loss of 7 OTf^- counterions $[M–7OTf^-]^{7+}$. M = **FeCu-cube** = $(C_{408}H_{264}Cu_6Fe_8N_{72})(OTf)_{16}$.

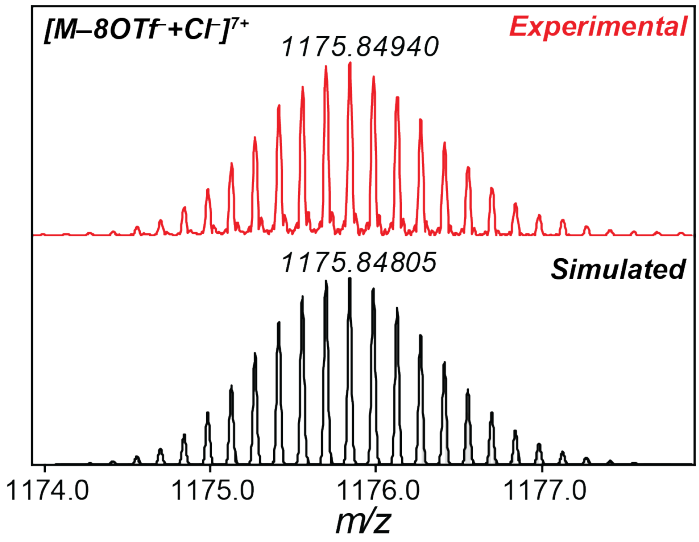

Figure S4. The 7+ peak in Figure S2. (top) Experimental data, (bottom) simulated spectrum with loss of 8 OTf^- and gain of 1 Cl^- counterions $[M–8OTf^-+Cl^-]^{7+}$. M = **FeCu-cube** = $(C_{408}H_{264}Cu_6Fe_8N_{72})(OTf)_{16}$.

UV-Vis Spectroscopy:

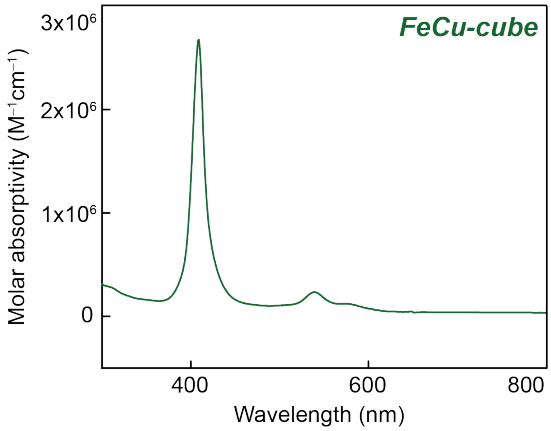

Figure S5. UV-Vis spectrum of **FeCu-cube** in CH_3CN.

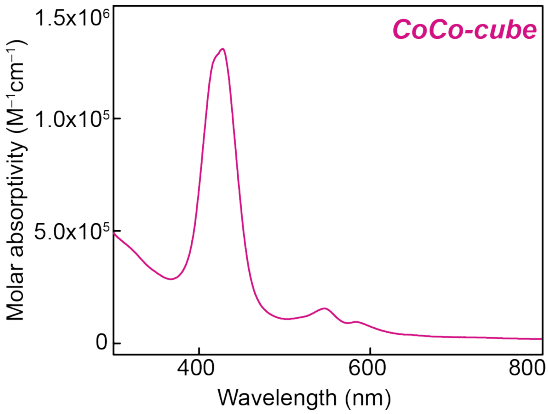

Figure S6. UV-Vis spectrum of **CoCo-cube** in CH_3CN.

Infrared Spectroscopy:

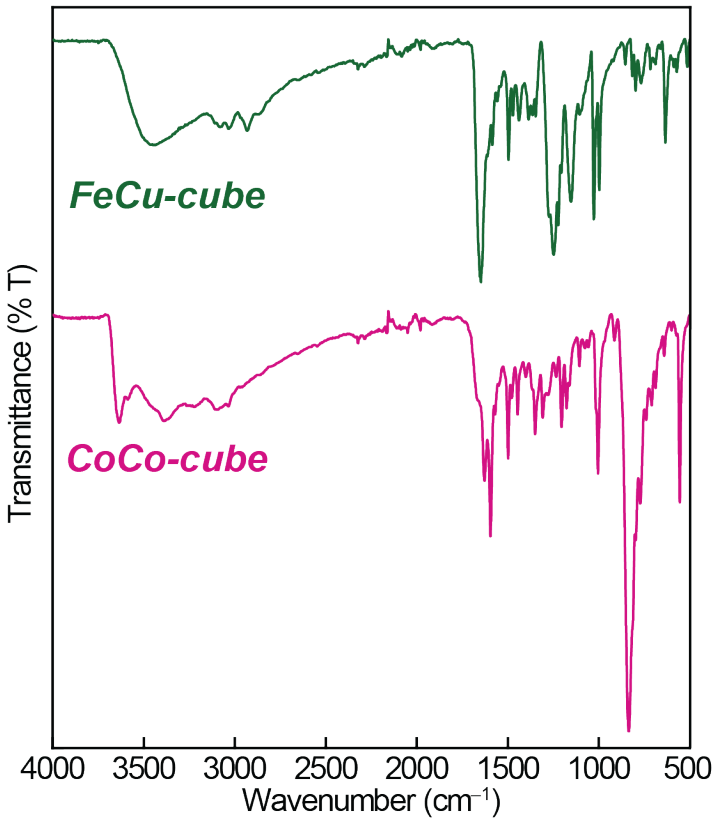

Figure S7. ATR-FTIR spectra of (top) **FeCu-cube** and (bottom) **CoCo-cube**.

Electrochemical Characterization

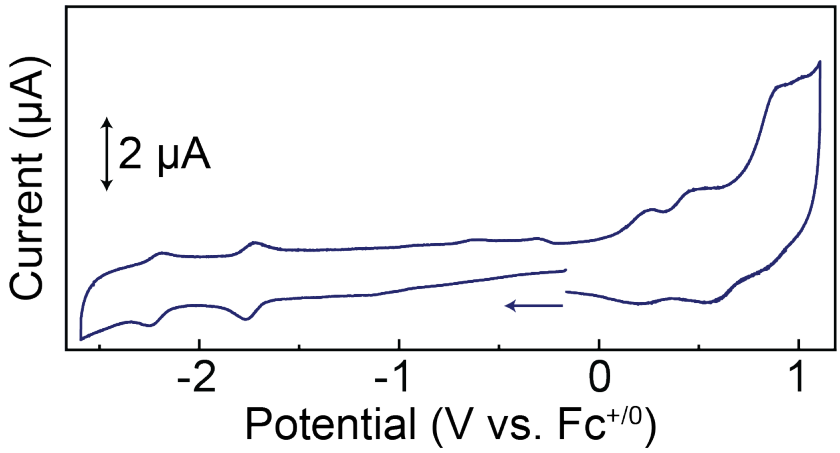

Figure S8. Cyclic voltammogram of CuTAPP (0.1 mM) in CH_3CN with 100 mM $TBAPF_6$.

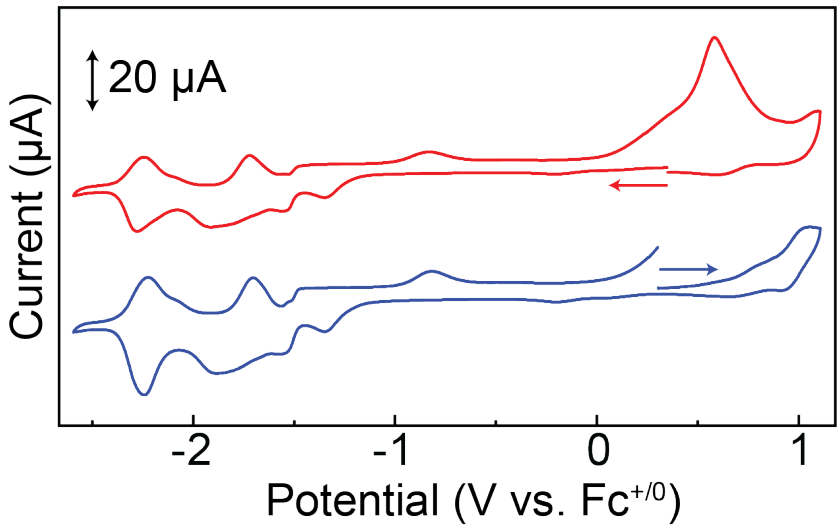

Figure S9. Cyclic voltammogram of **FeCu-cube (**0.1 mM) in CH_3CN with 100 mM $TBAPF_6$. (top) Red trace shows the first cycle when scanned reducing first. (bottom) Blue trace shows the first cycle when scanned oxidizing first. Notably, the large oxidation event observed in the red trace is absent until reducing potentials are scanned.

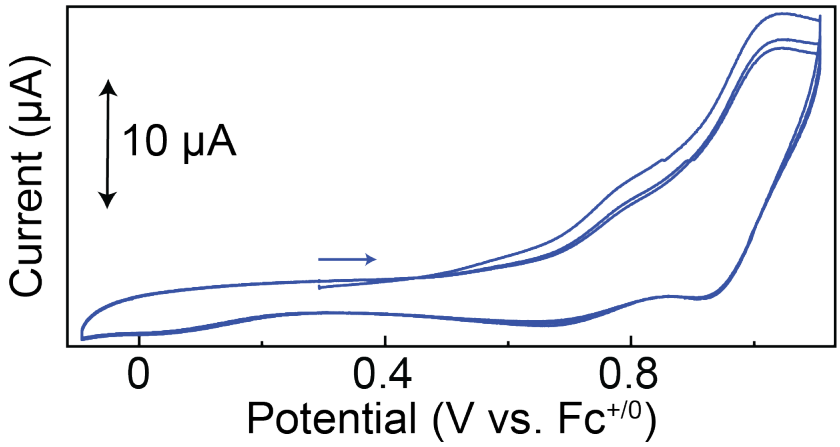

Figure S10. Cyclic voltammogram of **FeCu-cube (**0.1 mM) in CH_3CN with 100 mM $TBAPF_6$, cycled scanning only oxidizing potentials.

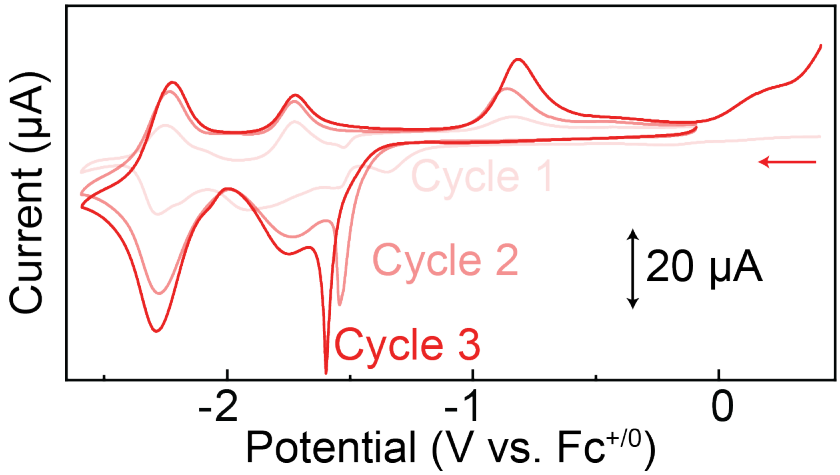

Figure S11. Cyclic voltammogram of **FeCu-cube (**0.1 mM) in CH_3CN with 100 mM $TBAPF_6$, cycled scanning only reducing potentials.

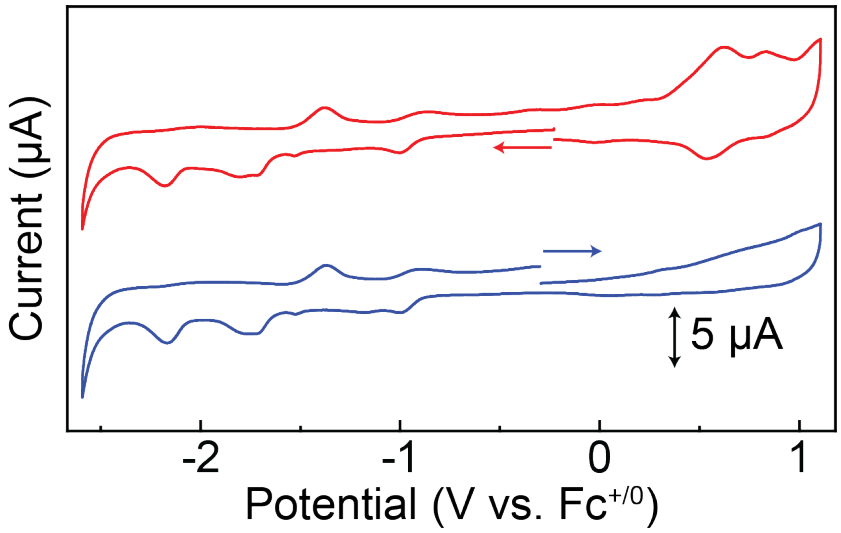

Figure S12. Cyclic voltammogram of **CoCo-cube (**0.05 mM) in CH_3CN with 100 mM $TBAPF_6$. (top) Red trace shows the first cycle when scanned reducing first. (bottom) Blue trace shows the first cycle when scanned oxidizing first. Note, the oxidation events observed in the red trace are absent until reducing potentials are scanned.

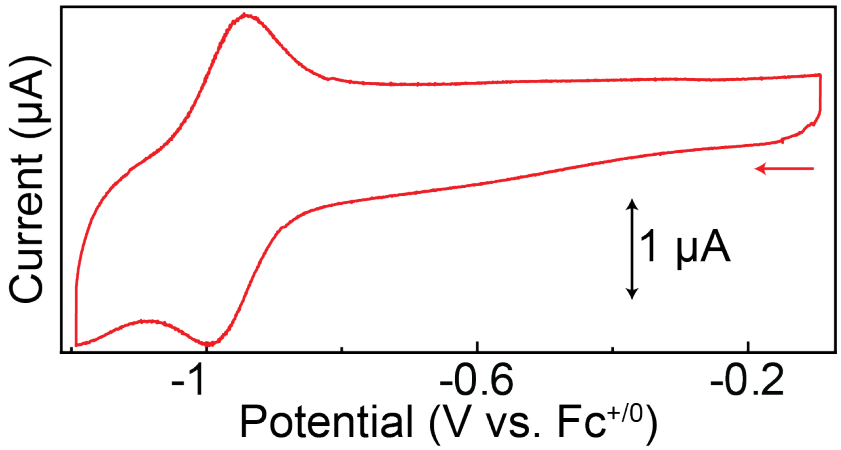

Figure S13. Cyclic voltammogram of **CoCo-cube** (0.05 mM) in CH_3CN with 100 mM $TBAPF_6$, isolating first reduction event (porphyrin Co(II/I) couple).

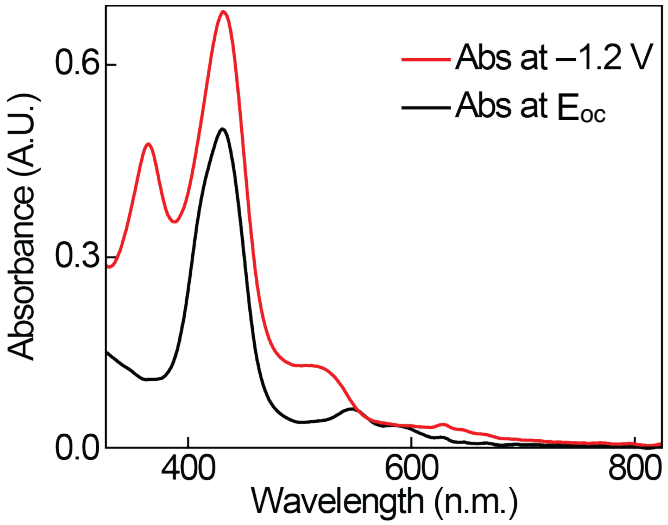

Figure S14. UV-Vis spectroelectrochemical study of the first reduction event of **CoCo-cube**. Platinum mesh electrode held at – 1.2 V vs. $Fc^{+/0}$. The growth of the band at ~360 and 520 nm are consistent with the formation of a Co(I) porphyrin species.

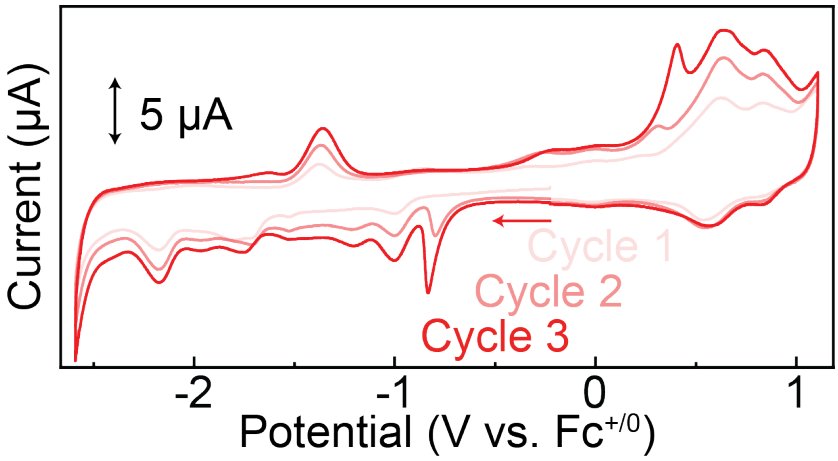

Figure S15. Cyclic voltammograms of **CoCo-cube (**0.05 mM) in CH_3CN with 100 mM $TBAPF_6$, cycled 3 times.

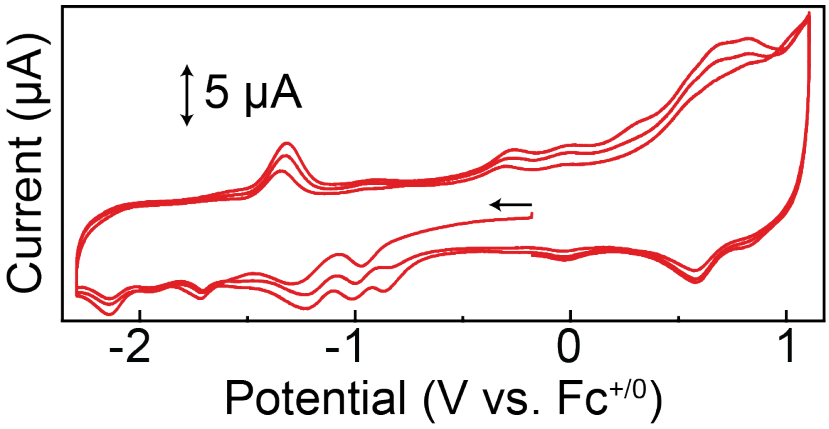

Figure S16. Cyclic voltammograms of **CoCo-cube (**0.01 mM) in CH_3CN with 100 mM $TBAPF_6$, cycled 3 times at 300 mV/sec. Concentration was reduced and scan rate increased to reduce film formation; however, evidence of film formation persists.

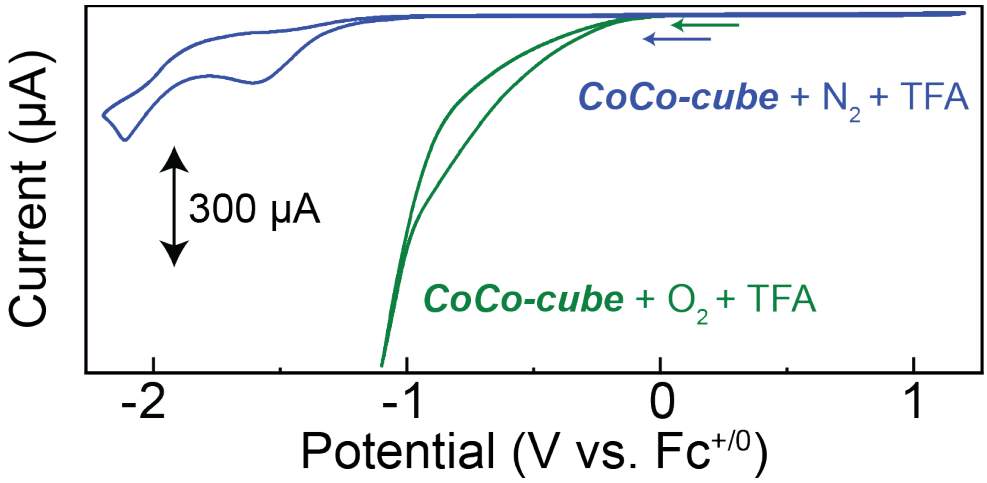

Figure S17. Cyclic voltammograms of **CoCo-cube (**0.05 mM) in CH_3CN with 100 mM $TBAPF_6$ and 100 mM TFA after sparging with N_2 (blue) and O_2 (green).

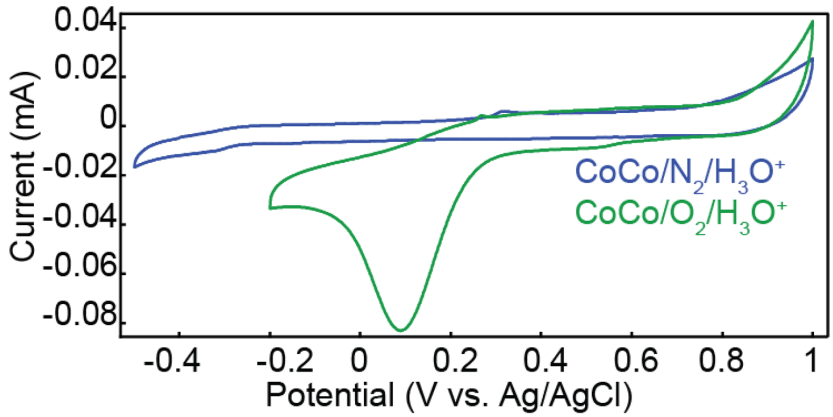

Figure S18. CV of heterogeneous catalyst ink of **CoCo-cube** deposited on a glassy carbon working electrode, in 0.5 M H_2SO_4, after sparging with O_2 (green trace), and N_2 (blue trace).

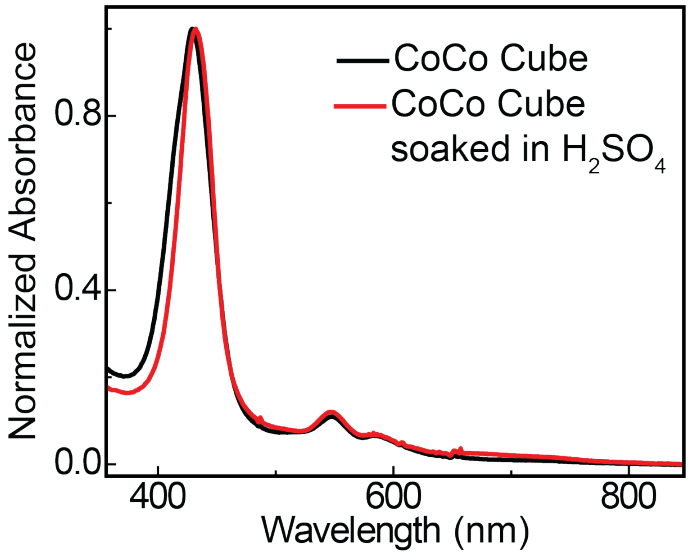

Figure S19. Acid stability study of **CoCo-cube** under catalytic conditions. Solid **CoCo-cube** was soaked in 0.5 M H_2SO_4, rinsed with water, isopropanol, and dissolved in acetonitrile.

As a control study, we synthesized *tris*(N-phenyl-pyridinaldimine)cobalt(II) hexafluorophosphate as a model complex for the nodes of the **CoCo-cube** following literature protocol:[1]

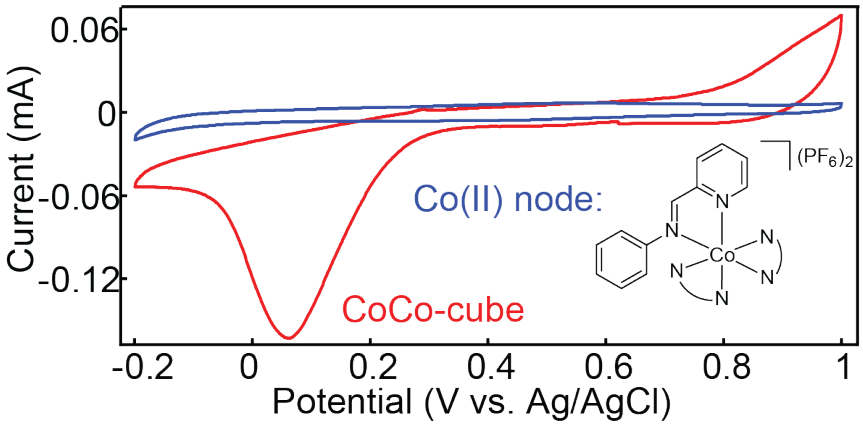

Figure S20. Heterogeneous CV of **CoCo-cube** and *tris*(N-phenyl-pyridinaldimine)cobalt(II) hexafluorophosphate deposited on a glassy carbon electrode under catalytic conditions (0.5 M H_2SO_4, saturated O_2).

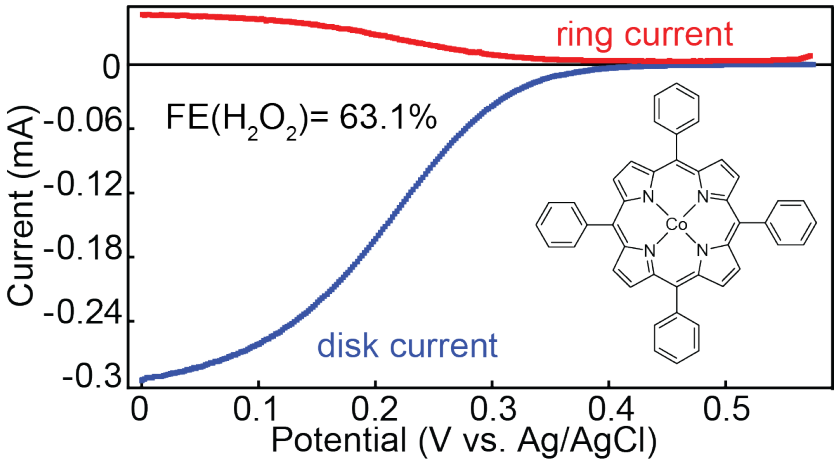

Figure S21. RRDE study of CoTPP as a model for the faces of the **CoCo-cube**. Films were formed identically to the **CoCo-cube** and analysis under identical conditions (0.5 M H_2SO_4, saturated O_2).

Koutecký–Levich Analysis and Selectivity:

$$\frac{1}{i} = \frac{1}{B}\omega^{-\frac{1}{2}} + \frac{1}{i_K} \qquad \textbf{(S1)}$$

Where i is the reductive current response due to ORR, B is the Levich constant, ω is the rotation rate in rad/sec, and i_K is the theoretical current that would pass absent mass transport effects (the kinetic current). The kinetic current is related to the heterogeneous electron transfer rate constant as follows:

$$i_K = nFAk_{het}[O_2]\Gamma_{cat} \qquad \textbf{(S2)}$$

Where n is the number of electrons transferred, determined by the Faradaic efficiency, F is Faraday's constant, A is the electrode surface area, $[O_2]$ is the dissolved concentration of O_2 in 0.5 M H_2SO_4, and Γ_{cat} is the ideal active site density, or moles of catalyst per unit area. The standard rate constant (k_s) is related to k_{het} by:

$$k_{het} = k_s e^{\frac{-\alpha F\eta}{RT}} \qquad \textbf{(S3)}$$

Where the exponential term contains α the transfer coefficient, F is Faraday's constant, R the gas constant, and T the temperature in Kelvin, and η is the overpotential.

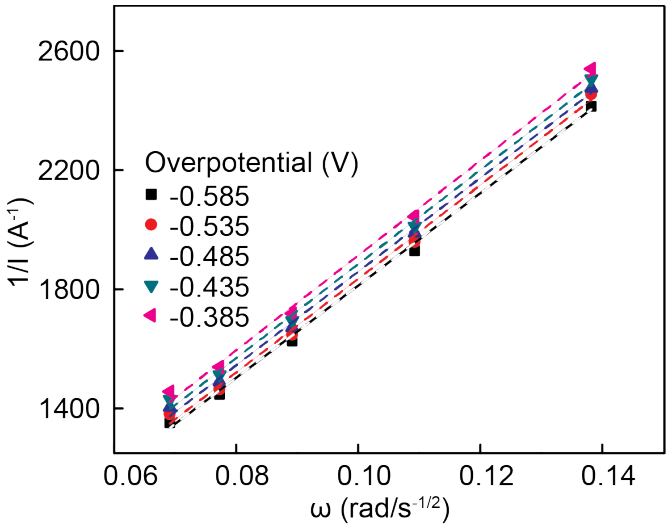

Figure S22. Plot of $1/i$ vs. ω at different overpotentials. Using Eq. 1, the y-intercepts at each overpotential can be related to a k_{het} with Eq. S2.

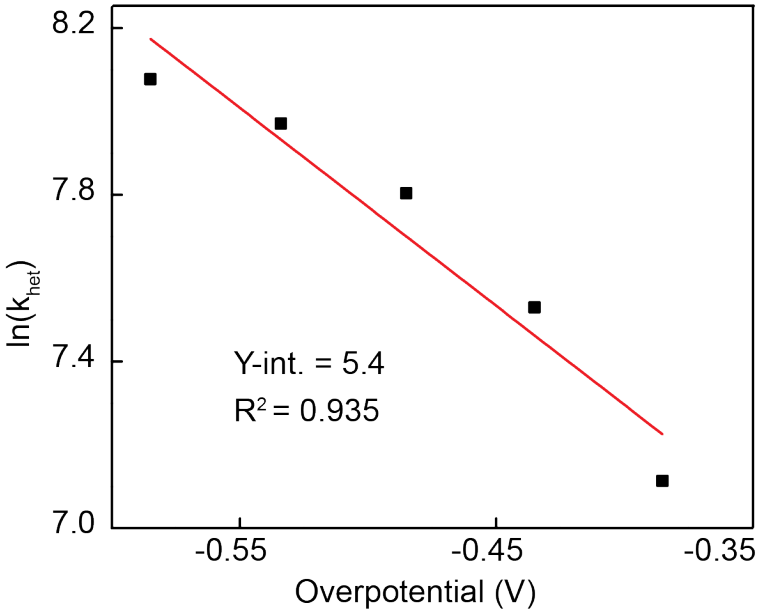

Figure S23. Plot of $\ln(k_{het})$ vs. overpotential. Using Eq. S3 the y-intercept will be the $\ln(k_s)$.

The following equation can be used to determine selectivity:

$$\%H_2O_2 = \frac{\frac{2i_{ring}}{N}}{i_{disk} + \frac{i_{ring}}{N}} \bullet 100 \qquad \textbf{(S4)}$$

Where i_{ring} and i_{disk} refer to the ring and disk currents, respectively, and N is the collection efficiency (0.36), which was experimentally determined using $K_3[Fe(CN)_6]$.[2-3]

References

1. Riddell, I. A.; Smulders, M. M. J.; Clegg, J. K.; Hristova, Y. R.; Breiner, B.; Thoburn, J. D.; Nitschke, J. R., *Nature Chemistry* **2012,** *4,* 751-756.
2. Bard, A. J.; Faulkner, L. R., *Electrochemical Methods: Fundamentals and Applications*. Wiley: 2000.
3. Crawley, M. R.; Zhang, D.; Oldacre, A. N.; Beavers, C. M.; Friedman, A. E.; Cook, T. R., *J. Am. Chem. Soc.* **2021,** *143,* 1098-1106.